Erschienen in: Energy Procedia ; 77 (2015). - S. 75-82
https://dx.doi.org/10.1016/j.egypro.2015.07.012

Available online at www.sciencedirect.com

ScienceDirect

Energy Procedia 77 (2015) 75 – 82

Energy Procedia

5th International Conference on Silicon Photovoltaics, SiliconPV 2015

Comparison of BO Regeneration dynamics in PERC and Al-BSF solar cells

Axel Herguth[a]*, Renate Horbelt[a], Svenja Wilking[a], R. Job[b], Giso Hahn[a]

[a]*University of Konstanz, Department of Physics, 78457 Konstanz, Germany*
[b]*Münster University of Applied Sciences, Dept. of El. Engineering and Computer Science, 48565 Steinfurt, Germany*

Abstract

Boron-oxygen related lifetime degradation is a severe problem for high-efficiency solar cells as the applied concepts like PERC suffer strongly from the observed lifetime degradation. However, these efficiency losses can be avoided via the Regeneration process eliminating the harmful defects. Within this contribution the effect of device structure on Regeneration kinetics is investigated. It is found that PERC-type cells regenerate faster than full area Al-BSF-type cells. It is pointed out why PERC-type cells benefit from an injection level effect. But this effect is not the only reason for the accelerated Regeneration. By means of especially adapted PERC cells, which do not benefit from the injection level advantage, it is shown that a second hydrogen containing layer on the rear has a positive influence, too, probably due to an increased hydrogenation of the silicon bulk.

© 2015 The Authors. Published by Elsevier Ltd. This is an open access article under the CC BY-NC-ND license (http://creativecommons.org/licenses/by-nc-nd/4.0/).
Peer review by the scientific conference committee of SiliconPV 2015 under responsibility of PSE AG

Keywords: PERC; Al-BSF; BO-degradation;BO-Regeneration

1. Introduction

Nowadays, mainly two cell concepts can be found in silicon wafer based solar cell mass production: the rather old-fashioned full area Al-BSF and the rather new PERC (passivated emitter and rear) concept, both realized on typically boron doped p-type substrates. Both concepts may suffer from a degradation of bulk lifetime due to boron-oxygen related defects [1-5]. A possible way to permanently avoid this degradation is the so-called Regeneration

* Corresponding author. Tel.: +49 7531 882967; fax: +49 7531 883895.
E-mail address: axel.herguth@uni-konstanz.de

Konstanzer Online-Publikations-System (KOPS)
URL: http://nbn-resolving.de/urn:nbn:de:bsz:352-0-312019

1876-6102 © 2015 The Authors. Published by Elsevier Ltd. This is an open access article under the CC BY-NC-ND license (http://creativecommons.org/licenses/by-nc-nd/4.0/).
Peer review by the scientific conference committee of SiliconPV 2015 under responsibility of PSE AG
doi:10.1016/j.egypro.2015.07.012

process invented in 2006 [6-10], in which harmful active meta-stable defect species are converted into an inactive, stable species. Recent investigations have shown [11-14] that hydrogen seems to play a key role in this process and therefore all constraints influencing the hydrogenation of the silicon bulk are likely to influence Regeneration kinetics. The change of concept from full area Al-BSF-type to PERC-type is therefore expected to influence Regeneration kinetics. Within this contribution, full area Al-BSF as well as PERC-type cells with similar front side but differing on the rear side are processed to investigate the influence of hydrogen on Regeneration kinetics in both concepts. In addition, the general role of injection level is discussed.

2. Structural properties of full area Al-BSF and PERC-type solar cells

In principle, full area Al-BSF and PERC-type cells on p-type substrates differ only in one point: the rear side contact. While in the classical full area Al-BSF concept Al paste is screen-printed directly on the rear side of the silicon substrate and the contact forms on the full area during the firing process, the rear side of PERC-type cells is passivated by a dielectric layer or stack. The contact to the substrate is achieved by opening the dielectric only locally (e.g. via laser ablation or wet chemistry), printing Al-paste on the full area and forming the actual contact sites in the locally opened/ablated areas during the firing process. It is worth to have a closer look on the microscopic contact formation to understand the later shown dependency on the firing process.

During the firing process of both cell types, Al liquefies around 660°C and dissolves silicon from the substrate. [15] The maximum concentration of Si in the Al melt depends on the one hand on the solubility (determined by peak temperature) reached during the short firing step and on the other hand on the geometry of the contact [16]. During cool down, the solubility of Si in Al decreases and Si re-crystallizes preferably at the substrate/melt interface incorporating Al as dopant according to the Al/Si binary phase diagram [17]. Thus a p^+-doped region gradually forms with a doping level locally equaling the solubility of Al in Si. More precisely, the Al dopant concentration within the re-crystallized region is not constant as the re-crystallization takes place at decreasing temperatures and, as the solubility of Al in Si decreases with temperature, the incorporated Al concentration decreases as well leading to a concentration gradient within the re-crystallized p^+ doped region [18]. It also means that starting the re-crystallization process at higher temperatures leads to stronger doped regions. The residual liquid Al/Si melt finally solidifies at the eutectic temperature of 577°C on top of the Al-doped Si region forming the actual contact [15]. It should be mentioned here that state-of-the-art Al screen-printing pastes are enriched also with B which is also incorporated during re-crystallization and, due to a high solubility of B in Si, boosts the doping effect well beyond the solubility limit of Al [19].

The doping level reached in local contacts is typically lower than that of full area contacts at the same peak temperature because the dissolved Si diffuses laterally in the Al melt away from the contact site. Thus the Si concentration in the vicinity of the solid/melt interface is lower and re-crystallization starts at a lower temperature. In consequence, the maximum Al concentration in the re-crystallized region falls below the value reached in full area alloyed cells. Adding Si to the Al paste counteracts this effect [16].

The doping step between substrate ($\sim10^{16}$ cm^{-3}) and p^+-region ($>10^{18}$ cm^{-3}) results in the well known electric back surface field (BSF), screening the actual Al/Si interface for the electrons. The effectiveness of screening depends (besides other entities) on the height of the doping step with higher steps being beneficial. In consequence, higher peak temperatures, leading to a stronger Al (and B) doped Si region, decrease the effective surface recombination velocity (SRV) of the rear contact. Typical effective SRV values for Al-BSFs range from 300-700 cm/s depending on peak firing temperature, Al paste composition, and substrate doping. Both cell concepts rely to a certain degree on this effect, the full area Al-BSF type cell (as the name states) to 100%, the PERC-type cell only to 5-10% depending on the exact rear contact area fraction, meaning the area weighed Al-BSF in the local contacts only contributes 25-50 cm/s (SRV_{BSF} 500 cm/s) plus the area weighed SRV of the passivated area (90-95%). The actually achieved effective rear side SRV depends therefore rather on the passivation quality of the dielectric layer/stack after the firing step than on the Al-BSF and thus the firing conditions have to be optimized especially with respect to the performance of the dielectric layer/stack. It should be remarked here that by far not every dielectric layer/stack endures higher temperatures even though hydrogen is also known to passivate the c-Si/dielectric interface. Especially the often used AlO_x passivation layers are known to be temperature sensitive [20-23].

3. General dependencies for Regeneration kinetics

Regeneration takes place at elevated temperatures, typically 100-200°C, and simultaneous charge carrier injection either by illumination or biasing. The Regeneration reaction is thermally activated thus higher temperatures speed up the process [6,7,10]. Furthermore, it is known that the Regeneration reaction speeds up with rising injection level. This can be done by the experimenter by simply increasing the illumination intensity or injected bias current [8,10].

However, the achieved injection level depends on some sample (fixed) properties. For example it matters if the solar cell is short-circuited or open circuited under illumination [8,9], as the operation condition controls the achieved injection level as well. Surface recombination also plays a major role as it may impose a lifetime limitation for the sample as a whole if the correlated surface lifetime comes close to or lies below the bulk lifetime. In this context it is often forgotten that even an emitter layer acts as a passivation layer [24].

In addition to temperature and injection level, both adjustable in the Regeneration process, hydrogen was found to play a key role in the regeneration reaction [11-14]. From various experiments mainly performed on lifetime basis one may conclude that the overall amount of hydrogen, typically originating from hydrogenated dielectrics like SiN_x:H, in the silicon bulk essentially determines the time constant of the Regeneration process at a given temperature and injection level [12-14].

4. Decoupling the different influences on Regeneration kinetics

As at least the two known factors of injection level and hydrogen content of the silicon bulk determine the Regeneration time constant, i.e., the time needed for almost complete recovery of the minority carrier lifetime, these two influences have to be decoupled to study which factor affects the investigated cell concepts to a certain degree.

4.1. Injection level

The minority carrier injection level Δn in a p-type solar cell under illumination or external biasing can be estimated according to the non-equilibrium mass action law

$$n \cdot p = (n_0 + \Delta n) \cdot (p_0 + \Delta p) = n_i^2 \cdot \exp\left({qV}/{kT} \right)$$

where n and p are the non-equilibrium electron and hole density, n_0 and p_0 the thermal equilibrium densities, n_i the intrinsic carrier density, kT the thermal energy (in eV), q the elementary charge, and qV the local quasi-Fermi level splitting (local voltage). The estimated injection level Δn at 300 K is exemplarily depicted in Fig. 1 (left). As the cell is typically illuminated and not connected for Regeneration, V equals the open circuit voltage V_{oc} of the solar cell which is by far a better measurable entity compared to the injection level Δn. The achievable V_{oc} of a solar cell can in turn be estimated according to the one diode model

$$V_{oc} = {kT}/{q} \cdot \ln\left({j_{sc}}/{j_0} + 1 \right)$$

with j_{sc} being the short circuit current density and j_0 the diode's saturation current density. The correct value of j_{sc} is not of upmost importance as the derivative dV_{oc}/dj_{sc} features only a small value < 1 mV/(mA/cm²). The diode saturation current density j_0 is the sum of emitter j_{0e} and volume j_{0b} saturation current density. As remarked above, the front side of both cell concepts is identical and thus j_{0e} may be assumed identical. The bulk's contribution j_{0b} is given for an infinite bulk with acceptor concentration N_A by

$$j_{0b} = \frac{qDn_i^2}{N_A} \cdot \frac{1}{L} \qquad L_{eff} = L \cdot \frac{1 + {SL}/{D} \cdot \tanh\left({d}/{L}\right)}{{SL}/{D} + \tanh\left({d}/{L}\right)}$$

which can be adapted for the finite bulk by replacing the diffusion length $L = \sqrt{D\tau_b}$ by an effective diffusion length L_{eff} which in turn includes the rear SRV S and the finite thickness d. In Fig. 1 (right) the expected V_{oc} at 300 K is plotted versus bulk lifetime as well as effective rear SRV assuming a j_{0e} of 150 fA/cm². In summary, V_{oc} is a measure of the achieved injection level Δn and is dominated by both bulk lifetime τ_b and rear SRV S.

PERC-type solar cells typically benefit from a lower effective rear SRV in the range of 50-100 cm/s as compared to 300-700 cm/s for full area Al-BSF-type cells and therefore typically feature V_{oc} around 650-660 mV under STC which is roughly 20 mV higher than that of Al-BSF type cells. Thus the PERC concept typically exhibits a higher injection level under similar illumination conditions and, as the Regeneration rate increases with injection level, has the potential of a faster Regeneration process, at least at room temperature.

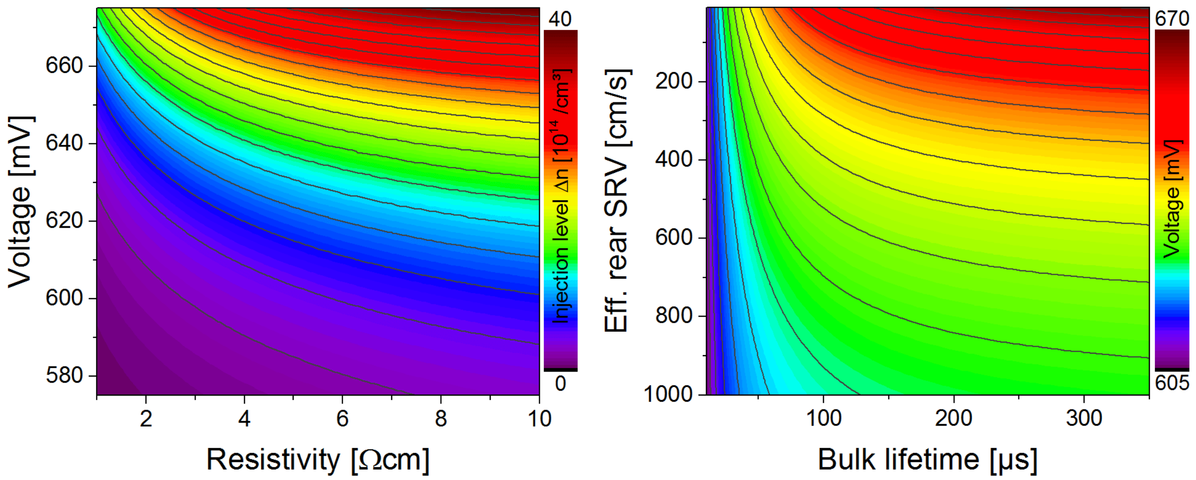

Fig. 1: (left) Estimated injection level Δn (scaled linearly) at 300 K present in a solar cell with certain base resistivity when a voltage is either generated by illumination or biasing. (right) Estimated open circuit voltage V_{oc} of a solar cell (scaled linearly) at 300 K in dependence of bulk lifetime and effective rear SRV assuming an emitter saturation current density j_{0e} of 150 fA/cm².

However, Regeneration takes place at elevated temperatures, e.g., 120-200°C, and arguing with V_{oc} (as a measure of injection level) determined at room temperature is somewhat misleading. The meaningful entity is V_{oc} measured at Regeneration temperature T_R (and under the applied illumination). Hence the question is how strong V_{oc} is decreased when raising the temperature. In general, the temperature coefficient dV_{oc}/dT of a solar cell may be approximated from the one diode model yielding

$$\left.\frac{dV_{oc}}{dT}\right|_T \approx -\frac{1}{T}\cdot\left(\frac{E_{go}}{q}-V_{oc}(T)\right) \qquad V_{oc}(T_R)=V_{oc}(25°C)+\int_{25°C}^{T_R}\frac{dV_{oc}}{dT}\cdot dT$$

using $j_0 \propto n_i^2 \propto T^3 exp\left(-E_g/kT\right)$ and E_{go} being the band gap of silicon at 0 K. In accordance to observations, solar cells exhibiting a higher V_{oc} at room temperature typically feature a better temperature coefficient dV_{oc}/dT and thus PERC-type cells not only exhibit a higher V_{oc} at room temperature, but also maintain their V_{oc} better than full area Al-BSF-type cells. Therefore, it can be concluded that PERC-type cells typically benefit from an increased injection level also promoted by a better temperature coefficient.

4.2. Hydrogen content

It is by far more complicated to investigate to what degree hydrogen plays a role in the different cell concepts. Four main aspects have to be taken into account: the hydrogen source capacity, the actual hydrogen amount released from the source into the silicon bulk, its distribution in the silicon bulk and the capability to confine the hydrogen in silicon bulk.

As probably all PERC-type cells exhibit a hydrogenated dielectric passivation layer or stack on the rear side, in most cases including a SiN_x:H layer, PERC-type cells feature not only a hydrogen source on the front side, but also on the rear side thus doubling virtually the hydrogen source capacity as compared to full area Al-BSF-type cells. Actually the hydrogen source capacity of the rear side dielectric is likely higher than that of the front side, because the passivation layer/stack on the front side serves also as anti-reflection coating and thus its thickness is defined by optimum optical transmission, while it can be chosen thicker on the rear side which also suppresses absorption losses in the metal above the dielectric layer/stack due to parasitic evanescent transmission through the dielectric. Thus the source capacity is often even more than doubled.

The amount of hydrogen released from the dielectric layers is determined mainly by the temperature profile used for firing screen-printed metal contacts. For example, at temperatures above approx. 650°C hydrogen is released from SiN_x:H with the release rate per volume element increasing strongly with rising temperature [14]. Thus the total released amount of hydrogen from the dielectric layer depends on the temperature/duration profile above 650°C, layer thickness and also layer composition. However, only a small fraction of the released hydrogen diffuses into the silicon bulk, the rest is lost to the ambient. How much hydrogen actually arrives in the silicon bulk depends again on temperature but also on layer composition and, in case of a dielectric stack, the capability of an interlayer to hinder diffusion or the capability of an outer layer to confine the released hydrogen. Fortunately, the often used thin AlO_x or SiO_x interlayers exhibiting only a few nanometers in thickness do not seem to act as significant diffusion barrier layers [13].

The distribution of hydrogen within the bulk is probably not a limiting factor as the diffusivity of hydrogen seems to be sufficiently high during the firing process to more or less evenly distribute hydrogen in the silicon bulk.

What might also play a role is the capability of the different cell concepts to confine the hydrogen within the bulk where it is needed for Regeneration. Especially in the full area Al-BSF concept hydrogen might get lost by either trapping at Al in the doped region or effusion through the Al contact. Even though this effect can occur also in PERC-type cells with local contacts, the small area fraction of rear side contacts should diminish this effect.

5. Experiment

In order to investigate experimentally the influence of hydrogen source capacity, release behavior and maybe trapping/effusion behavior in both cell concepts, Al-BSF and PERC-type solar cells were manufactured. Both groups were made of the same material (~1.3 Ωcm boron doped Cz-Si, ~180 µm thickness after processing) and received identical front side processing (alkaline texture, $POCl_3$-based emitter, SiO_x/SiN_x:H passivation/ARC stack, Ag screen-printed contacts). For the PERC group a SiO_x/SiN_x:H stack was created on the rear side and the dielectric stack was locally ablated in a line pattern by laser. The rear side of both groups was screen-printed with Al-paste and all cells were fired in an IR belt furnace. Several subgroups were defined each with a different set peak temperature and/or belt speed as shown in Table 1.

Table 1: Temperature set values for the different subgroups

Group	1	2	3	4	5	6	7
set peak T [°C]	800	+20	+40	+20	+40	+40	+60
belt speed	slow	slow	slow	medium	medium	fast	fast

As the experiment aims only at the hydrogen influence on Regeneration in different cell concepts, the influence of injection level (as discussed above) was countered in two ways: Firstly, the passivation quality of the dielectric stack on the rear side was deliberately chosen not optimized, so that the PERC-type cells in this experiment exhibit V_{oc} values even slightly below those of the Al-BSF-type cells in the annealed state. Secondly, the illumination (around 1 sun) during Regeneration (at 130°C, V_{oc} conditions, in-situ monitored until saturation, see Fig. 3) was adapted to yield approximately the same start/end voltage. Residual deviations lie in the range of 5 mV, their estimated influence is reflected in the error bars.

Prior to Regeneration treatment (~1 sun, 130°C), the samples were annealed (dark, ~200°C, 10 min) and subsequently degraded (0.1 sun, ~45°C, 48 h). Note that these steps are not needed for Regeneration to occur as during Regeneration conditions cells are degrading very fast and almost instantaneously compared to the time constant of Regeneration. After completed Regeneration step, the samples were exposed again to degradation conditions (0.1 sun, ~45°C) to check for incomplete Regeneration and then annealed again to check for other effects degrading the performance. After each stage the electrical parameters of the cells were determined under standard test conditions.

6. Results and interpretation

The V_{oc} values for both cell concepts and their subgroups at different stages of the experiment are shown in Fig. 2. As can be seen in the bar graphs, all subgroups could regain almost the complete voltage loss due to degradation via the Regeneration process; the regenerated V_{oc} of the PERC-type cells even exceeds the annealed value, to which all voltages in each subgroup were normalized. The voltage was stable after Regeneration within error margins on a high level and the final anneal hits almost perfectly the starting value.

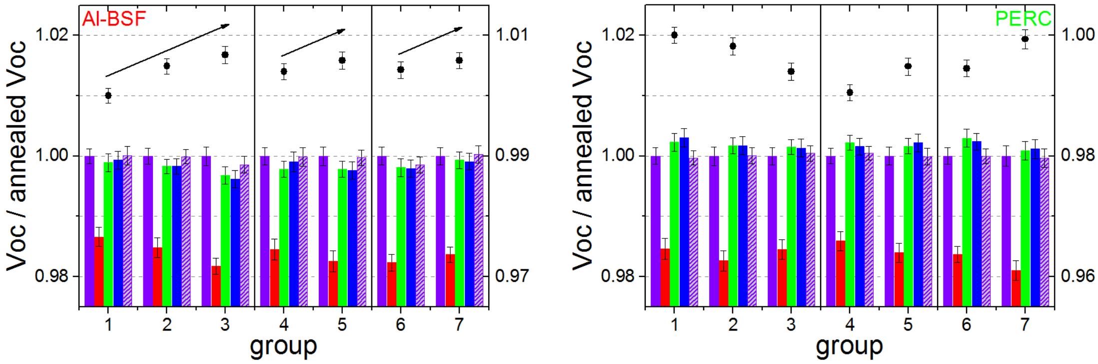

Fig. 2: V_{oc} changes at different stages of the experiment for the Al-BSF (left) and PERC-type cells (right). The bar graph shows V_{oc} values relative to the annealed V_{oc} value of each subgroup (left scale) at different stages: violet after annealing, red after degradation, green after Regeneration, blue after repeated degradation and violet striped after repeated annealing. The data points above show the annealed V_{oc} value relative to the annealed V_{oc} value of the first group (right scale).

The data points in Fig. 2 depict the achieved annealed V_{oc} values relative to the first group. For the full area Al-BSF-type cells a clear trend can be seen. Within the groups (1,2,3), (4,5) and (6,7) the relative V_{oc} increases. Within each of these groups the set temperature and hence also the achieved cell peak temperature increases. From group (1,2,3) to (4,5) the belt speed was increased and thus the samples had less time to heat up in the hot zone of the belt furnace. Comparing subgroups 2 and 4 (same set temperature, 2 slower than 4) subgroup 2 features a slightly higher V_{oc} than subgroup 4. The same holds for subgroups 3 and 6. This behavior seems to be perfectly in line with the expectations discussed in section 2: the higher the peak temperature, the better the field passivation, the better V_{oc} and therefore one can conclude that it is beneficial to fire full area Al-BSF-type cells rather hot.

For the PERC-type cells no clear trend is visible. The observed gains/losses in V_{oc} show neither significant improvement nor drastic deterioration of the rear side passivation. As it is the aim of this experiment to clarify the influence of hydrogen and, as the injection level effect rather disturbs and complicates the experiment, an almost insensitive rear surface passivation is beneficial here. However, one has to bear in mind, that a SiO_x/SiN_x:H passivation stack was used in this experiment which is less temperature sensitive as compared to the often used AlO_x/SiN_x:H passivation stacks.

During Regeneration treatment the evolution of V_{oc} was in-situ monitored starting from the degraded state and a single exponential fit was used to extract a specific time constant as depicted in Fig. 3 (left). The time constants for both cell types and each subgroup are shown in Fig. 3 (right).

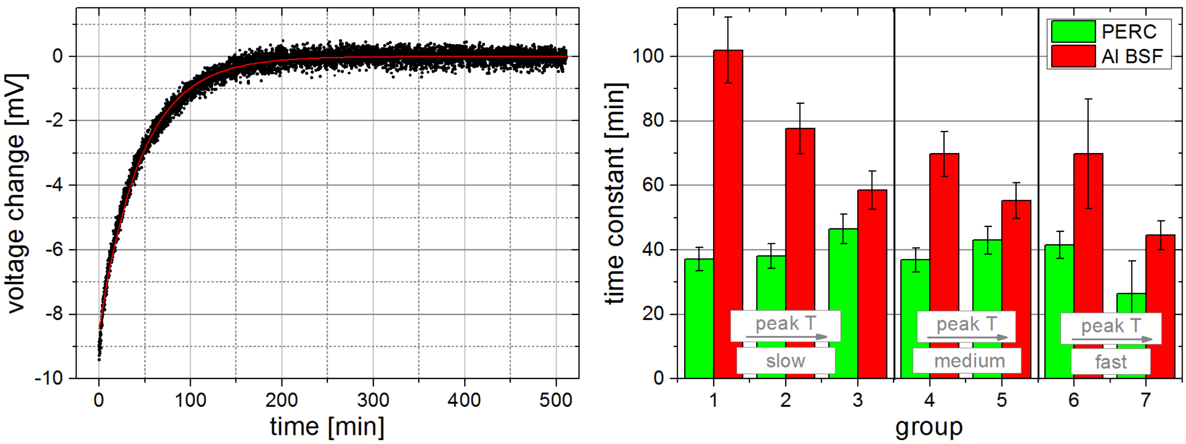

Fig. 3: (left) Exemplary in-situ measurement of the change in V_{oc} during Regeneration treatment at 130°C, ~1 sun illumination. A single exponential function (shown in red) was used to extract a time constant. (right) Comparison of the determined time constants for the different cell concepts and subgroups (see Table 1).

As can be seen, the time constants for both cell types differ beyond error margins. The PERC-type cells always exhibit shorter time constants irrespective of the firing conditions. Note again that the injection level effect was suppressed for this specific experiment and thus the observation cannot be ascribed to a generally higher injection level of typical PERC-type cells. Hence we credit this finding rather to the structural difference between the two cell concepts: the second hydrogen source on the rear side and the eased hydrogenation of the bulk during the firing step.

For the PERC-type cells no clear trend can be seen within the error margins. Hence we conclude that the different firing conditions applied within this experiment have no significant influence on the Regeneration behavior maybe because hydrogen is not the limiting factor for Regeneration due to an oversupply of hydrogen from the double sided, high capacity hydrogen source and/or a very homogeneous hydrogen distribution in depth.

In contrast, for the full area Al-BSF-type cells a clear trend can be seen. Within each group (1,2,3), (4,5) and (6,7) exhibiting rising set temperature the time constant decreases. Again changing the belt speed, e.g., from subgroup 3 to 4, alters the effectively reached peak temperature explaining the step in time constant between subgroups 3/4 and 5/6, respectively. We ascribe the acceleration of the Regeneration process with increasing temperature to better hydrogenation of the silicon bulk as more hydrogen is released from the SiN_x:H layer. It is also interesting to see that the gap between full area Al-BSF and PERC-type cells seems to close with increasing temperature. This might be interpreted in the way that hydrogenation, meaning distribution homogeneity and amount, is improved that much that hydrogen is also for full area Al-BSF type cells not a limiting factor any more.

However, it should be kept in mind that especially the PERC-type cells in this experiment were de-optimized and that Regeneration conditions were adapted in order to suppress the injection level effect. If this would have not been the case, meaning a generally higher injection level under constant illumination intensity for the PERC-type cells, the gap in time constant between both cell concepts would have been larger and would probably not close completely.

7. Conclusions

In good agreement with the results from Cascant et al. [25] it is found that PERC-type cells are prone to regenerate faster than full area Al-BSF-type cells. However, the results from this experiment show that not only the injection level effect, described here in theory, is responsible for the faster Regeneration of PERC-type cells as compared to full area Al-BSF-type cells, but that the additional hydrogen source layer on the rear side of the especially adapted PERC-type cells also contributes to this acceleration. The unclear trend with respect to the different applied firing conditions suggests that the double-sided hydrogen source might already oversupply the bulk. In contrast, the closing gap in time constant between the two cell concepts with increasing firing temperature suggests that this is not the case for full area Al-BSF-type cells.

Acknowledgements

Part of this work was financially supported by the German Federal Ministry for the Environment, Nature Conservation and Nuclear Safety (FKZ 0325450 and FKZ 0325581). The content of this publication is in the responsibility of the authors.

References

[1] Knobloch J, Glunz SW, Biro D, Warta W, Schäffer E, Wettling W, Solar cells with efficiencies above 21% processed from Czochraski grown silicon. Proc. 25th IEEE PVSC 1996; pp.405-408.
[2] Glunz SW, Rein S, Warta W, Knobloch J, Wettling W. Degradation of carrier lifetime in Cz silicon solar cells. Sol En Mat Solar Cells 2001; 65:219.
[3] Schmidt J, Cuevas A, Rein S, Glunz SW. Impact of light-induced recombination centres on the current-voltage characteristics of Czochraski silicon solar cells. Prog Photovolt: Res Appl 2001; 9:249
[4] Bothe K, Sinton R, Schmidt J. Fundamental Boron-Oxygen-related carrier lifetime limit in mono- and multicrystalline silicon. Prog Phtotovolt: Res Appl 2005; 13:287
[5] Bothe K, Schmidt J. Electronically activated boron-oxygen-related recombination centers in crystalline silicon. J Appl Phys 2006; 99:013701
[6] Herguth A, Schubert G, Kaes M, Hahn G. A new approach to prevent the negative impact of the metastable defect in boron doped Cz silicon solar cells. Proc. 4th WCPEC, 2006, pp.940-943
[7] Herguth A, Schubert G, Kaes M, Hahn G. Avoiding boron-oxygen related degradation in highly boron doped Cz silicon. Proc. 21st EU-PVSEC, 2006, pp.530-537
[8] Herguth A, Schubert G, Kaes M, Hahn G. Investigations on the long time behavior of the metastable boron-oxygen complex in crystalline silicon. Prog Photovolt: Res Appl 2008; 16:135
[9] Herguth A, Schubert G, Kaes M, Hahn G. Further investigations on the avoidance of boron-oxygen related degradation by means of regeneration. Proc. 22nd EU-PVSEC 2007, pp. 893-896
[10] Herguth A, Hahn G. Kinetics of the boron-oxygen related defect in theory and experiment. J Appl Phys 2010; 108:114509
[11] Münzer KA. Hydrogenated silicon nitride for Regeneration of light induced degradation. Proc. 24th EU-PVSEC, 2009, pp.1558-1561
[12] Wilking S, Herguth A, Hahn G. Influence of hydrogenated passivation layers on the Regeneration of boron-oxygen related defects. En Proc 2013; 38 pp. 642-648
[13] Wilking S, Herguth A, Hahn G. Influence of hydrogen on the regeneration of boron-oxygen related defects in crystalline silicon. J Appl Phys 2013; 113:194503
[14] Wilking S, Ebert S, Herguth A, Hahn G. Influence of hydrogen effusion from hydrogenated silicon nitride layers on the regeneration of boron-oxygen related defects in crystalline silicon. J Appl Phys 2013; 114:194512
[15] Huster F. Investigation of the alloying process of screen printed aluminium pastes for the BSF formation on silicon solar cells. Proc. 20th EU-PVSEC 2005, pp. 1466-1469
[16] Lauermann T, Fröhlich B, Hahn G, Terheiden B. Diffusion-based model of local Al back surface field formation for industrial passivated emitter and rear cell solar cells. Prog Photovolt: Res Appl 2015; 23(1):10-18
[17] Murray JL, McAlister AJ. The Al-Si system. Bulletin of alloy phase diagrams 1984; 5(1)
[18] Huster F. ECV doping profile measurements of aluminium alloyed back surface fields. Proc. 20th EU-PVSEC 2005, pp. 1462-1465
[19] Rauer M, Schmiga C, Glatthaar M, Glunz SW. Alloying from screen-printed aluminum pastes containing boron additives. IEEE J PV 2014; 3(1):206-211
[20] Benick J, Richter A, Hermle M, Glunz SW. Thermal stability of the Al_2O_3 passivation on p-type silicon surfaces for solar cell applications. Phys Stat Sol RRL 2009; 3, No. 7 – 8, 233– 235
[21] Vermang B, Loozen X, Allebé C, John J, Van Kerschaver E, Poortmans J, Mertens R. Characterization and implementation of thermal ALD Al_2O_3 as surface passivation for industrial Si solar cells. Proc. 24th EU-PVSEC 2009, pp.1051–1054
[22] Veith B, Werner F, Zielke D, Brendel R, Schmidt J. Comparison of the thermal stability of single Al_2O_3 layers and Al_2O_3 /SiN_x stacks for the surface passivation of silicon. En Proc 2011; 8:307–312
[23] Lauermann T. Integration von Hocheffizienzmerkmalen auf im Siebdruckverfahren metallisierte Solarzellen mittels funktioneller Strukturierung. PhD thesis University Konstanz 2013
[24] Wilking S, Engelhardt J, Ebert S, Beckh C, Herguth A, Hahn G.High speed Regeneration of BO-defects: Improving long-term solar cell performance within seconds. Proc. 29th EU-PVSEC 2014; pp.366-372
[25] Cascant M, Enjalbert N, Monna R, Dubois S. Influence of various p-type Czochralski silicon solar cell architectures on light-induced degradation and regeneration mechanisms. Proc 29th EU-PVSEC 2014; pp.2570-2573